I&EC research
Industrial & Engineering Chemistry Research

Article

pubs.acs.org/IECR

Evaluation of Novel Ceria-Supported Metal Oxides As Oxygen Carriers for Chemical-Looping Combustion

Ali Hedayati,[†] Abdul-Majeed Azad,*[,‡] Magnus Rydén,[§] Henrik Leion,[†] and Tobias Mattisson[§]

[†]Department of Chemical and Biological Engineering, Chalmers University of Technology, SE-412 96 Göteborg, Sweden
[‡]Department of Chemical Engineering, The University of Toledo, Ohio 43606-3390, United States Toledo, United States
[§]Department of Energy and Environment, Chalmers University of Technology, SE-412 96 Göteborg, Sweden

ABSTRACT: Oxygen carrier particles consisting of 60 wt % copper, iron, or manganese oxide supported on 40 wt % ceria (CeO_2) or gadolinia doped-ceria ($Ce_{0.9}Gd_{0.1}O_{1.9}$) have been manufactured and examined as oxygen carrier materials for chemical-looping combustion (CLC). Unlike conventional support materials, such as alumina (Al_2O_3), these ceria-based support materials are active under prevailing conditions in the fuel reactor and have the ability to participate in redox reactions. The oxygen carrier materials were synthesized via extrusion and were examined by successive oxidation and reduction cycles in a bench-scale fluidized bed reactor made of quartz. The experiments were conducted at 900 and 925 °C for copper-based materials, and at 950 °C for iron- and manganese-based materials. Methane or syngas (50% CO and 50% H_2) using a flow rate of 900 mL/min for Cu-based materials and 450 mL/min for Mn- and Fe-based materials was used as the fuel. For all experiments, 15 g of oxygen carrier was used. The oxidation was performed with a gas mixture of 5% O_2 and 95% N_2. The results show that CeO_2 and $Ce_{0.9}Gd_{0.1}O_{1.9}$ are viable support materials for the oxides of copper and iron. Moreover, the active particles supported on $Ce_{0.9}Gd_{0.1}O_{1.9}$ were more reactive compared to those supported on CeO_2. CH_4 was completely converted to CO_2 and H_2O by CuO supported on $Ce_{0.9}Gd_{0.1}O_{1.9}$, while the conversion of CH_4 for Fe_2O_3 supported on $Ce_{0.9}Gd_{0.1}O_{1.9}$ was as high as 90%. Ceria-supported Mn_3O_4 particles showed poor performance when CH_4 was used as fuel. Syngas was fully converted to CO_2 and H_2O by all the oxygen carriers synthesized and examined in this work. The ability of CuO and Mn_2O_3 to release O_2 in gas phase when fluidized in inert background was also investigated; in the case of copper oxide, substantial oxygen release was observed. Analysis of fresh and used particles by X-ray diffractometry did not reveal the formation of any unexpected phases. All particles showed good fluidization properties with low attrition and little tendency toward agglomeration.

1. INTRODUCTION

1.1. Chemical-Looping Combustion. Chemical-looping combustion (CLC) is an emerging technology for conversion of carbonaceous fuels into heat with inherent CO_2 capture. In CLC, fuel is oxidized with oxygen provided by solid oxygen carrier particles, rather than with O_2 direct from air. In principle, chemical-looping combustion consists of two interconnected reactors, an air reactor and a fuel reactor. In the air reactor, oxygen depleted particles are exposed to a flow of air, whereby they are oxidized with O_2 according to reaction 1:

$$O_2(g) + 2Me_xO_{y-1} \leftrightarrow 2Me_xO_y \quad (1)$$

The oxidized particles are then transported to the fuel reactor, in which a fuel is used to reduce the particles, while forming CO_2 and H_2O in the process, see reaction 2:

$$(2n + m)Me_xO_y + C_nH_{2m} \leftrightarrow (2n + m)Me_xO_{y-1} + mH_2O + nCO_2 \quad (2)$$

Reduced particles are transferred back to the air reactor for reoxidation by reaction 1, and the cycle can begin again. The sum of reactions 1 and 2 is combustion of fuel with O_2, and the net energy released is the same as for conventional combustion. In this manner, the fuel is oxidized without mixing with N_2 from air. Therefore, the flue gas consists mainly of CO_2 and H_2O undiluted with N_2. Chemical-looping combustion has several attractive features. Most importantly, since cooling of the off-gases is all that is needed to obtain an almost pure CO_2 stream, chemical-looping combustion offers an ideal technology for the generation of heat and power with inherent CO_2 sequestration. A schematic description of the process is shown in Figure 1.

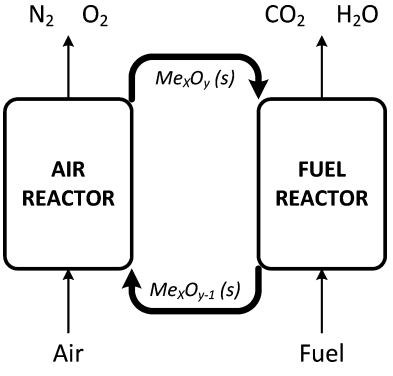

Figure 1. Schematic description of the chemical-looping combustion process.

Received: January 18, 2012
Revised: July 15, 2012
Accepted: August 24, 2012
Published: August 24, 2012

   dx.doi.org/10.1021/ie300168j | *Ind. Eng. Chem. Res.* 2012, 51, 12796−12806

Most often, the chemical-looping combustion reactors are designed as interconnected fluidized beds, with oxygen-carrier particles used as bed material and continuously transferred between the reactors. The general principles were laid out as early as in the 1950s by Lewis and Gilliland,[1] but most of the work concerning the technology has been conducted in the past decade. The progress in the field has been reviewed recently by Hossain and De Lasa,[2] Fang et al.,[3] Lyngfelt,[4] and Moghtaderi.[5]

One notable variant of the chemical-looping combustion concept is chemical-looping with oxygen uncoupling (CLOU).[6] Here an oxygen carrier material with the propensity to release gas phase O_2 directly into the fuel reactor is used. In this case, though the net reaction in each reactor vessel is identical with chemical-looping combustion, the fuel oxidation mechanism is different. In ordinary chemical-looping combustion, oxidation takes place mainly via gas−solid reaction. Consequently, if a solid fuel such as coal or biomass is used, it has to be gasified in order to be able to react with the oxygen carrier. In contrast, in the CLOU-process, solid fuel can react directly with the gas phase O_2 released by the carrier and hence, does not need to be gasified. Experiments by Mattisson et al. and by Leion et al. have shown that oxidation of solid fuels, such as petroleum coke can be ∼45 times faster in the CLOU-process using CuO as oxygen carrier.[6,7] This is significant in comparison to the normal chemical-looping combustion (CLC) process, where gasification of solid fuel with steam is the rate limiting step.

1.2. Oxygen Carrier Materials. The availability of feasible oxygen carrier materials is one of the main challenges in the development of CLC and CLOU processes. Some of the prerequisites in the choice of oxygen carrier are adequate rates of oxidation and reduction, thermodynamic propensity, which allows high conversion of fuel into CO_2 and H_2O, and good resistance toward attrition, fragmentation, and agglomeration. The oxygen carrier should also preferably be inexpensive and environmentally benign. Other relevant criteria include high melting point and high content of oxygen[8,9] that enable and facilitate reactions 1 and 2. The most commonly used oxygen carrier materials are the oxides of copper (CuO-Cu_2O−Cu), iron (Fe_2O_3−Fe_3O_4), manganese (Mn_2O_3−Mn_3O_4), and nickel (NiO−Ni).

CuO has favorable properties, such as high reactivity during reduction, typically resulting in full conversion of gaseous hydrocarbon fuels, for example, CH_4. Unlike most of the other alternatives, the reaction of CuO in the fuel reactor with hydrocarbon fuels is exothermic, which could be advantageous from a heat balance point of view. The use of CuO in CLC has been examined by several research groups. Gayan et al.[10] investigated the effect of different supports on the behavior of CuO-based oxygen carriers. Chuang et al.[11] systematically investigated the CuO−Al_2O_3 particles synthesized in three different ways and concluded that particles made through coprecipitation showed the best operational behavior. De Diego et al. and Forero et.al[12,13] designed 10 and 0.5 KW_{th} chemical-looping reactors and operated them for 100 h with CH_4 as fuel, and for 40 h with syngas as fuel, respectively, utilizing CuO−Al_2O_3 carrier particles prepared by impregnation.

Fe_2O_3 is readily available because of its large natural abundance, low price, and favorable thermodynamic properties. Abad et al.[14] have reported 10−94% conversion of CH_4 with Fe_2O_3 supported on Al_2O_3 in a small circulating fluidized bed reactor in the temperature range of 800 to 950 °C. In a study of fluidization aspects of Fe_2O_3-supported on Al_2O_3 at 950 °C using CH_4 as fuel, Cho et al.[15] found that defluidization is inhibited as long as Fe_3O_4 is not reduced to FeO in the fuel reactor. Rydén et al.[16,17] and Leion et al.[18] have examined synthetic iron-based and iron-containing waste materials as oxygen carrier for chemical-looping combustion, using a reactor and methodology similar to the one used in this study.

Mn_3O_4 is prone to react with many potential support materials such as Al_2O_3, SiO_2, and TiO_2. However, Johansson et al.[19] investigated Mn_3O_4 supported on calcia-, magnesia-, and ceria-stabilized ZrO_2 and reported good reactivity during reduction with CH_4. The magnesia-stabilized ZrO_2 support exhibited the best properties in terms of reactivity and stability. This oxygen carrier has also performed well in a small, continuously operated, reactor for 70 h as reported by Abad et al.[20]

NiO shows very high reactivity with gaseous fuels but unfortunately has some major drawbacks, such as high toxicity and high price. Furthermore, complete conversion of CO and H_2 into CO_2 and H_2O is not possible because of thermodynamic constraints, as noted by Jerndal et al.[8] Because of this, NiO-based carriers were not investigated in this study.

Oxygen-carrier materials for chemical-looping with oxygen uncoupling are required to have similar properties as those employed in conventional CLC; in addition, they also need to be thermodynamically capable of taking up and releasing gas-phase O_2 under relevant conditions. Fe_2O_3 and NiO do not satisfy this requirement, as they can not release gas phase O_2. The most widely and thoroughly examined oxide pair is CuO−Cu_2O, which has been shown to work very well for CLOU application.[6,7] On the basis of the reliable phase diagram of the pseudobinary Mn_2O_3−Mn_3O_4 system, this oxide pair is also amenable to CLOU application. However, the experiments with unmodified manganese oxides typically show either no or very low O_2 release in the temperature regime of interest and relevance. This is likely due to the rather low temperature range for the release of appreciable amount of O_2 for this oxide pair, which results in slow reaction kinetics. On the other hand, several Mn-bearing systems such as mixed iron−manganese oxides[21,22] and calcium manganate[23,24] provided better results than those based on pure Mn_2O_3−Mn_3O_4.

It is a common practice to support and use the active oxygen carrier on an inert material. The inert support helps to provide mechanical integrity to the particles during the redox process; it can also increase the porosity and surface area of the particles, thus indirectly improving its reactivity. The commonly used support materials are typically refractory ceramics with high melting points, such as Al_2O_3, ZrO_2, and $MgAl_2O_4$. Support materials are typically inert and do not participate nor contribute actively toward the fuel oxidation.

1.3. CeO_2 as Support Material for Oxygen Carrier Particles. Though significant strides have been made in the area of oxygen carriers in recent years, there is still room for improving the material systems and their performance. The objective of the present work is to achieve these goals by introducing the concept of a chemically active, rather than inert, support material. Since the redox attributes of the solid oxygen carriers play pivotal roles in chemical-looping processes, one could anticipate better performance if the support also possessed facile redox properties and could act as a minor but additional oxygen carrier. This would accentuate the agility by which a composite of the support and oxygen carrier would perform in the air as well as in the fuel reactor. However, one of the important prerequisite of such support would be the

dx.doi.org/10.1021/ie300168j | Ind. Eng. Chem. Res. 2012, 51, 12796−12806

complete reversibility of its oxygen exchange behavior in the two reactors.

One potential active support materials is cerium dioxide (CeO_2) also known as ceria, which is in use extensively in three-way catalysts for oxidizing CO and unburnt hydrocarbons and reducing nitrogen oxides in the exhaust stream of automobiles before they are released to the environment.[25] The choice of CeO_2 is based on its unusual but highly benign characteristics. For example, while Al_2O_3 is a common support for a number of catalysts in oil refining and in CLC because of its high thermal and chemical stability, there is a great deal of rationale for using CeO_2 supports in chemical-looping combustion. CeO_2 is commercially used in catalytic converters as a support for three-way catalysts, and it is well-known for its high oxygen storage capacity and easy reducibility because of its facile $Ce^{III} \leftrightarrow Ce^{IV}$ equilibrium. CeO_2-based materials are quite active and stable both in reducing and oxidizing atmospheres in high-temperature regimes compared to other conventional support systems. Utilization of CeO_2 as a support for common oxygen carriers for direct application in chemical looping systems for combustion of carbonaceous fuels is a new and promising concept in the light of the known behavior of CeO_2.

CeO_2 when nominally doped with 10−20 mol % of Gd_2O_3 (GDC) or ZrO_2 (ZDC), imparts additional stability to the support. The aliovalent ion doping also provides higher temperature stability and an increased oxygen storage capacity, resulting in an increase in oxygen vacancies which contributes to an increase in reducibility of the CeO_2, as well with a concomitant increase in its ionic conductivity.[25] The envisaged advantages of the CeO_2-supported oxygen carriers over the ones that are currently in use are higher activity, higher oxygen capacity, and larger oxygen ratio because of the participation of the support material in reactions 1 and 2.

This paper therefore investigates oxygen carrier particles consisting of 60 wt % copper, iron, or manganese oxide supported on 40 wt % ceria (CeO_2) or gadolinia-doped ceria ($Ce_{0.9}Gd_{0.1}O_{1.9}$). The particles have been synthesized via extrusion and examined as oxygen carrier materials for chemical-looping combustion (CLC).

2. EXPERIMENTAL SECTION

2.1. Manufacturing of Oxygen Carrier Particles. Oxygen carrier particles were manufactured in two stages. First, powder of CuO (97%), Mn_2O_3 (99%), or Fe_2O_3 (98%), all from Alfa-Aesar and with an average grain size ∼46 μm (325 mesh), was mixed with pure ceria (CeO_2, from Alfa-Aesa) or 10 mol % gadolinia doped-ceria ($Ce_{0.9}Gd_{0.1}O_{1.9}$, from NexTech Materials) in the weight ratio of 60:40. Each material composition was made in two batches (100 g per batch).

For this, the powders of oxygen carriers (CuO, Mn_2O_3, or Fe_2O_3) and CeO_2 or $Ce_{0.9}Gd_{0.1}O_{1.9}$ were weighed and mixed. The mixture was transferred to a 1-L pear-shaped distillation flask with 400 g of water, which was placed in a programmable 20-L water bath. The aqueous slurry was thoroughly mixed and homogenized in a Buchi R-110 rotary evaporator unit that was interfaced with a Buchi vacuum pump (V-710), a programmable Buchi vacuum controller (V-850) and a Buchi recirculating chiller (F-105). The rotary evaporator was operated by the 20/40/60 rule, 20 °C being the cooling water temperature in the chiller, 40 °C the boiling temperature of the water used as solvent at the reduced pressure, and 60 °C being the bath temperature. The rotary evaporator operation was initiated at relatively low vacuum level, and as the evaporation continued, the vacuum level was increased gradually. This pressure modulation varied from system to system. The duration of the evaporation was about 2 h for each 100 g batch, which ensured thorough mixing and uniform homogenization of the powders. After removal of about 2/3 of the water, a concentrated and viscous, albeit smooth, flowing slurry was obtained. The slurry was poured into a shallow Pyrex pan and dried at 150 °C in an air oven overnight. The dried soft cakey mass was then crushed and ground to a homogeneous powder.

The resulting powders were used to manufacture oxygen carrier particles by extrusion. For this, 170 g of powder of each formulation was weighed. It was converted into pliable dough. The procedure was as follows. The powder was mixed manually in a wide-mouthed plastic container with 10 g of poly vinyl alcohol with an average molecular weight of 25000 from Alfa-Aesar as binding agent, 2 g of soluble starch $(C_6H_{10}O_5)_n$ from Merck as auxiliary binder, and 2 g of LAROSTAT 519 (a quaternary ammonium salt; PPG Industries, IL) to increase the flux properties of the mixture. Next, 4 g of 1 M ammonium hydroxide as peptizing agent and 40 g of water was added. The somewhat wet mixture was then transferred to a food processor for mixing and homogenization. More water, typically 20−24 g in steps of 4 and 2 g batches, was gradually added as the ingredients were mixed mechanically, with intermittent stirring with plastic spatula, until pliant and flexible dough of desired plasticity suitable for extrusion was obtained. The total amount of water varied between 60 and 64 g, depending upon the formulation of the composite powder.

The dough was transferred to a hand-held single-screw extruder and squeezed to form strands of the ceramic component. This process (i) helped in avoiding the fine dust formation when the powder was directly transferred to the food processor for mixing and (ii) yielded the most optimum strands. This procedure proved to be optimal in producing the dough for reproducible extrusion. In the case of large batches, a more efficient mechanical mixer would be needed.

The strands were collected on a stainless steel sheet and dried in an air oven at 200−220 °C overnight. The dried extrudates were then transferred to high density alumina crucibles which were placed in a programmable muffle furnace and calcined in air at 950 °C for 6 and 12 h, or at 1100 °C for 6 h, using the temperature−time profile shown in Figure 2.

The first stage of calcination process is performed using a rather slow ramp rate, which is done to promote interparticle binding by the softening and plastic flow of the various polymeric components at low temperature. The second stage of soaking at 500 °C, called binder burnout, facilitated the removal

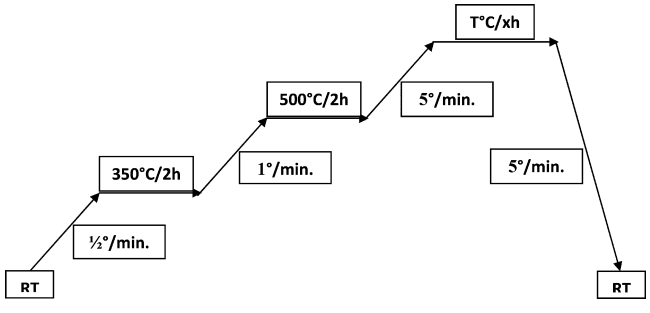

Figure 2. Temperature−time schedule used for the processing of carrier extrudates.

dx.doi.org/10.1021/ie300168j | Ind. Eng. Chem. Res. 2012, 51, 12796−12806

of carbonaceous and other gaseous compounds (mostly as CO_2, H_2O, and N_2), without compromising the physical structure of the spaghetti-like extruded strands. The final stage of calcination was meant for imparting densification and adequate strength to the composite carrier particles.

The calcined extrudates were sieved through stainless steel screens to yield particles in the range of 125−180 and 180−250 μm. In most of the cases, the frequency of the shaker cleaved the extrudates, making the particle screening through mesh simple. In the case of relatively hard materials, occasional dry ball-milling using alumina jar and alumina milling balls was required.

The oxygen carriers fabricated and used in this study are listed in Table 1. For the sake of brevity, the acronyms assigned to each formulation, will be used throughout the paper, to identify the formulation.

Table 1. Composition and Thermal History of the Oxygen Carriers Investigated in This Work

system	composition (wt/wt ratio)	ID	calcination history
$CuO-CeO_2$	60:40	COC	950 °C/6 h
$CuO-Ce_{0.9}Gd_{0.1}O_{1.9}$	60:40	COGDC	950 °C/12 h
$Fe_2O_3-CeO_2$	60:40	FOC1	950 °C/6 h
$Fe_2O_3-CeO_2$	60:40	FOC2	950 °C/12 h
$Fe_2O_3-Ce_{0.9}Gd_{0.1}O_{1.9}$	60:40	FOGDC	950 °C/6 h
$Mn_2O_3-CeO_2$	60:40	MOC	1100 °C/6 h

2.2. Particle Characterization. For each of the manufactured composite formulations, the crushing strength and bulk density of the fresh particles were carefully measured. Systematic phase analysis of the fresh, as well as the reduced and oxidized particles was carried out by X-ray diffraction (Siemens, D5000 Diffractometer) with CuK_α radiation.

The crushing strength was measured as the force required for fracturing particles within the size range 180−250 μm, using a digital force gauge (Shimpo, FGN-5). An average of measurements on about 30 particles was taken as the representative strength. The crushing strength was found to be less than 0.5 N for some of the samples, which may be too soft for use in a full scale application of the process. However, in the present study, this did not cause any problem, such as defluidization or attrition in the reactor, as determined by the pressure drop over the bed. Nonetheless, for use in a full scale plant, the crushing strength of the particles would probably need to be increased; this could be done by either increasing the temperature or length of the calcinations step.

2.3. Experimental Setup. The experiments were carried out in a batch fluidized-bed reactor made of quartz which was 870 mm long and had an inner diameter of 22 mm. A porous quartz plate was placed at a height of 370 mm from the bottom. The reactor temperature was measured with chromel-alumel (type K) thermocouples sheathed in inconel-600 clad located about 5 mm below and 25 mm above the plate. Honeywell pressure transducers with a frequency of 20 Hz were used to measure pressure differences over the bed. A schematic description of the experimental setup used in this investigation is shown in Figure 3.

2.4. Test Protocol. In a typical experiment, 15 g of the oxygen carrier particles was placed onto the porous plate. The reactor was placed inside a vertically split furnace and the experiment was initiated by heating the reactor to 900 °C. In some cases, test temperatures of 925 and 950 °C were also used. During heat-up, the oxygen carrier particles were fluidized with a gas mix of 5% O_2 and 95% N_2 to ensure full oxidation of the particles prior to the experiments. The use of 5% O_2 was aimed at being close to the expected condition at the air reactor's outlet in a real-world combustor and also to obviate large temperature increase during the exothermic oxidation.

When the desired temperature was reached, the experiment was initiated. To investigate the performance of the material, the particles were exposed to successive reduction and oxidation periods. Methane or syngas consisting of 50% H_2 and 50% CO was used as a fuel for reduction. Methane was chosen since the largest portion of natural gas is CH_4. The reason for using syngas of the specified composition was to mimic the fuel composition produced by gasification of solid fuels, such as coal or biomass. Oxidation was performed with 5% O_2 in N_2, for reasons explained above. To prevent the mixing of reducing and oxidizing gases, pure N_2 was injected for 60 s between every reduction and oxidation sequence.

For the initial reactivity tests, the carrier particles were exposed to a minimum of three reduction−oxidation cycles to assess the reproducibility and reliability of the process, as well as the reversibility characteristics of the oxygen carriers. The

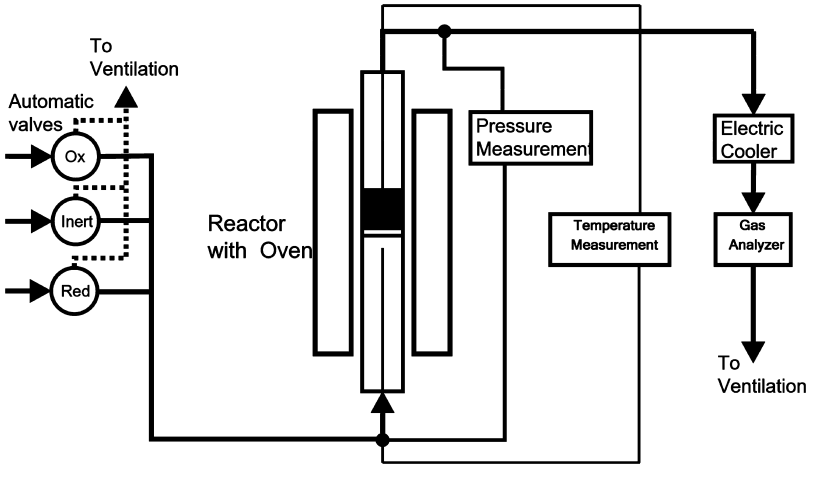

Figure 3. Schematic description of the experimental setup used in this investigation.

dx.doi.org/10.1021/ie300168j | Ind. Eng. Chem. Res. 2012, 51, 12796−12806

Table 2. Test Conditions Employed for Evaluating the Oxygen Carriers Developed in This Work

	nitrogen (N_2)		methane (CH_4)		syngas (CO/H_2)		5% O_2 in N_2	
oxygen carrier	flow rate (mL/min)	duration (s)	flow rate (mL/min)	duration (s)	flow rate (mL/min)	duration (s)	flow rate (mL/min)	duration (s)
COC	1200	60	900	12			1200	until fully oxidized
COGDC	600	60	900	12			1000	until fully oxidized
FOC1	600	60	450	20	450	80	900	until fully oxidized
FOC2	600	60	450	20	450	80	900	until fully oxidized
FOGDC	600	60	450	20	450	80	900	until fully oxidized
MOC	600	60	450	20	450	80	900	until fully oxidized

reduction time for individual material was calculated on the basis of flow rate and the maximum amount of oxygen available in each case for reaction with CH_4 or syngas and adjusted accordingly. The oxidation time was kept long enough to allow complete regeneration of the carriers. The reactor was purged with nitrogen for 360s, both before and after the fuel cycles and, after the full oxidation of the particles, to examine their oxygen uncoupling behavior. A summary of the experimental variables used in this work is presented in Table 2.

Different flow rates were used for each period to achieve conditions of stable fluidization of the particles in the reactor. In comparison to the previous experiments using a similar reactor setup,[16−18] the inert gas flow rates were higher in this work. In the case of copper-based particles, these high flows were needed also in the fuel cycle to maintain stable fluidization and avoid agglomeration in the bed. It is well established that the minimum flow of fluidization of a certain kind of particles is a function of properties, such as density, size distribution, and sphericity. Since the particles examined in this study were fabricated by extrusion, which resulted in denser and larger particles of less than spherical geometry compared to those manufactured for example by spray drying or freeze granulation, the need for slightly higher gas flow in the present case was not unexpected.

2.5. Data Analysis. The exit gas stream from the reactor was led into a condenser to remove water; hence, all measurements are on dry gases, the composition and flow rate of which was determined on a volumetric basis by a Rosemount NGA-2000 analyzer, which measured the concentration of O_2, CO_2, CO, CH_4, and H_2 as well as the total volumetric gas flow. An example of the time-dependent concentration profile for various gases and that of the total outlet flow rate is shown in Figure 4. The vertical dashed lines represent the reduction period during, which the fuel (methane) was streamed. Nitrogen was introduced as a purge gas before and after the reduction period.

The reactivity of a given oxygen carrier is quantified in terms of gas yield (γ_{red}) and is defined as the fraction of fully oxidized fuel divided by the carbon containing gases in the outlet stream, which in this work are CO_2, CO, and CH_4.

$$\gamma_{red} = \frac{x_{CO_2}}{x_{CH_4} + x_{CO_2} + x_{CO}} \tag{3}$$

Here x_i denotes the composition of the respective gas, obtained from measured concentration in the gas analyzer.

The theoretical oxygen capacity of a given oxygen carrier is defined in terms of the oxygen ratio (R_o), as the fraction of theoretical maximum mass change to the mass of the fully oxidized carrier as follows:

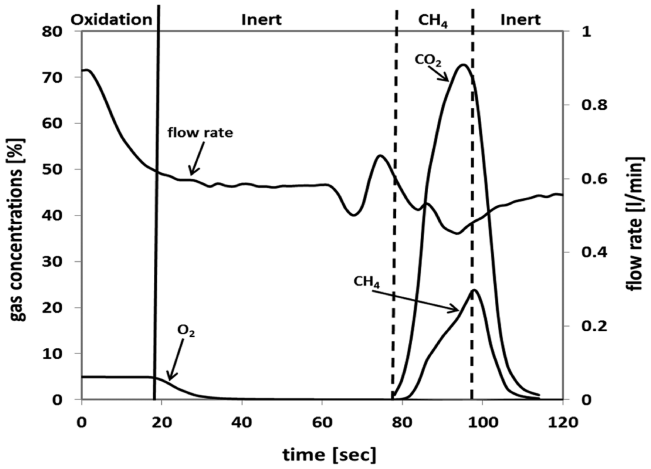

Figure 4. Time-dependent concentration and flow rate profile during a typical reduction for **FOGDC** carrier particles at 950 °C.

$$R_o = \frac{m_{ox} - m_{red}}{m_{ox}} \tag{4}$$

where m_{ox} and m_{red} are the mass of the oxygen carrier in fully oxidized and reduced state, respectively. The mass-based conversion of the oxygen carrier (ω) is defined as

$$\omega = \frac{m}{m_{ox}} \tag{5}$$

where m is the actual mass of the carrier. Equations 6 and 7 are employed for calculating ω as a function of time during the reduction period from the measured concentrations of various gaseous species in the gas analyzer for CH_4 and syngas cycles, respectively:

$$\omega_i = \omega_{i-1} - \int_{t_0}^{t_1} \frac{\dot{n}_{out} M_o}{m_{ox}} (4X_{CO_2} + 3X_{CO} - X_{H_2}) dt \tag{6}$$

$$\omega_i = \omega_{i-1} - \int_{t_0}^{t_1} \frac{\dot{n}_{out} M_o}{m_{ox}} (2X_{CO_2} + X_{CO} - X_{H_2}) dt \tag{7}$$

Here, ω_i is the instantaneous conversion at time i, ω_{i-1} the conversion in the preceding instant, t_0 and t_1 the initial and final time of measurement, M_0 the molecular weight of oxygen, and $\dot{n}_{out}$ is the molar flow rate of the gas at the reactor outlet after water removal.

3. RESULTS AND DISCUSSION

3.1. Oxygen Carrier Properties. For copper and iron based materials, the XRD results of fresh samples were in agreement with the phases present in the initial raw materials. Neither any new phases formed nor any phase transformation

dx.doi.org/10.1021/ie300168j | Ind. Eng. Chem. Res. 2012, 51, 12796−12806

was observed in the carriers calcined at different temperatures or for different durations. For the manganese-based particles, Mn_2O_3 had decomposed into Mn_3O_4 during calcination, which is in accordance with the thermodynamic prediction made by Metselaar et al.[26] The phase analysis on fresh samples is summarized in Table 3 and their relevant physical characteristics are given in Table 4.

Table 3. Phase Analysis of the As-Prepared Samples

oxygen carrier	phases identified
COC	CuO, CeO_2
COGDC	CuO, $Ce_{0.9}Gd_{0.1}O_{1.9}$
FOC	Fe_2O_3, CeO_2
FOGDC	Fe_2O_3, $Ce_{0.9}Gd_{0.1}O_{1.9}$
MOC	Mn_3O_4, CeO_2

Table 4. Physical Characteristics of the Oxygen Carriers Investigated in This Work

oxygen carrier	ID	size range (μm)	crushing strength (N)	apparent density (kg/m^3)
CuO−CeO_2	COC	180−250	0.33	2380
CuO−$Ce_{0.9}Gd_{0.1}O_{1.9}$	COGDC	180−250	0.33	3366
Fe_2O_3−CeO_2	FOC1	125−180	1.21	2610
Fe_2O_3−CeO_2	FOC2	180−250	0.84	2410
Fe_2O_3−$Ce_{0.9}Gd_{0.1}O_{1.9}$	FOGDC	125−180	0.49	1946
Mn_2O_3−CeO_2	MOC	180−250	0.85	3165

3.2. O_2 Release in Inert Environment. The ability of the oxygen carriers to release gas-phase oxygen was also investigated in this work. As seen from Figure 5, O_2 concentration does not drop to zero when the reactor containing copper-based carriers is fluidized with N_2. This is ascribed to the spontaneous decomposition of CuO into Cu_2O, releasing gas phase molecular O_2 via the so-called CLOU effect

$$4CuO \leftrightarrow 2Cu_2O + O_2(g) \quad (8)$$

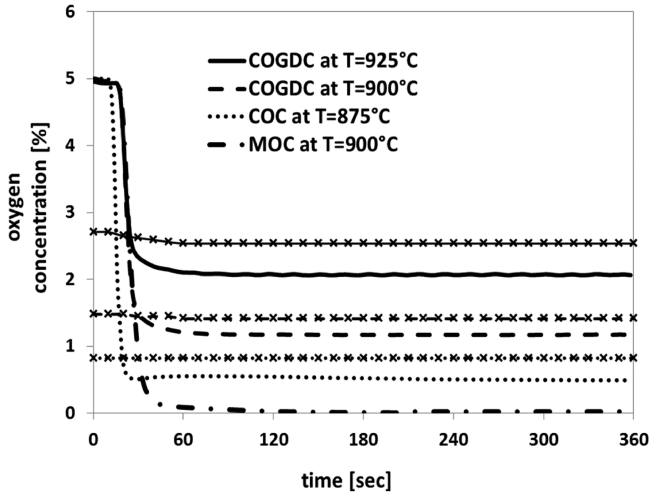

Figure 5. O_2 release from different Cu-based oxygen carriers during fluidization in inert background. For comparison, the equilibrium O_2 concentration value is included (×).

The amount of O_2 generated depends on the equilibrium partial pressure of O_2 over CuO−Cu_2O at a given temperature. The computed equilibrium O_2 concentrations are 2.4% at 925 °C, 1.4% at 900 °C, and 0.8% at 875 °C. The equilibrium oxygen partial pressure at the temperature measured in the bed of oxygen carriers is included in Figure 5. The equilibrium data were computed using the HSC Chemistry 6.1 software. As can be seen, the measured oxygen concentration in each case is somewhat lower but satisfactorily close to the anticipated value in the entire range of temperature of measurement (viz., 875−925 °C). The difference between the measured concentration and the equilibrium concentration could be due to the nature of the flow in the batch fluidized bed, with gas flow both in the emulsion and bubble phases. If there is a limitation to the mass-transfer between these two phases, one would expect a lower concentration at the outlet of the reactor.

As stated above, the decomposition of Mn_2O_3 to Mn_3O_4 with concomitant release of gaseous O_2 is possible for manganese-based oxygen carriers, but no such O_2 release was observed for the MOC particles, see Figure 5. The likely reason for this is that fresh MOC particles had Mn_3O_4 as active phase because of their calcination at higher temperatures, as can be seen from Table 3. As per the Mn−O phase diagram, oxidation of Mn_3O_4 to Mn_2O_3 is favored at low temperature. Additional experiments were conducted at 800 and 850 °C, but no O_2 release was seen at these temperatures either. Obviously, even lower temperatures would be needed to oxidize the particles to Mn_2O_3 under the conditions used in this study. No gaseous O_2 release could be expected from iron-based particles, and none was observed.

3.3. Activity of CeO_2. To assess the feasibility of ceria being a participating support, pure CeO_2 was tested under the experimental conditions described above at 900 and 950 °C. The results show that pure CeO_2 has the propensity to convert syngas into CO_2, as seen from Figure 6, though it did not release gaseous oxygen during N_2 purge (no CLOU behavior). This is expected in the light of the well-established reversible redox behavior of ceria under reducing conditions. The

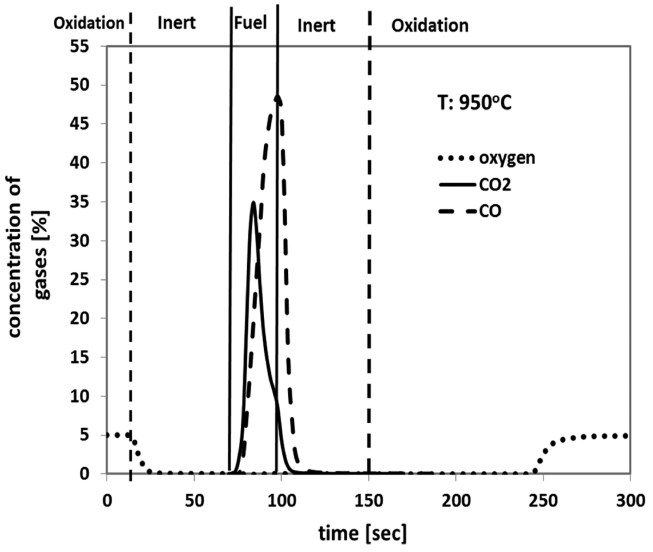

Figure 6. Concentration profiles of various gaseous components in the exit stream at 950 °C using syngas as fuel with pure **CeO_2** as the oxygen carrier.

dx.doi.org/10.1021/ie300168j | *Ind. Eng. Chem. Res.* 2012, 51, 12796−12806

conversion to CO_2 is incomplete, conforming to the thermodynamic predictions.[8]

The vertical lines in Figure 6 represent the time at which different reaction cycles actually began. The solid vertical lines, for example, represent the reduction period (25 s) during which syngas was purged. The dashed line on the right identifies the spot on the time-axis where oxidation cycle began. As stated earlier, nitrogen was purged for 60 s between the reduction and the subsequent oxidation cycle, to flush out the reactor of remnant fuel and the resulting gaseous products. It is evident that during the oxidation cycle (100 s), the reduced ceria consumed O_2 fully in a stream of 5% O_2 in N_2. Results were quite similar with experiments at 900 °C except that the fuel conversion was slightly lower and the CO_2 concentration peaked at 28% as opposed to 35% at 950 °C.

These observations pertaining to the fuel reduction capability of CeO_2 and facile oxygen uptake during oxidation cycle, demonstrate that CeO_2 is active in the temperature range of 900−950 °C. Moreover, no carbon deposition was detected during the fuel cycle and the activity of CeO_2 was not affected by successive redox cycles, which is a clear evidence of its robustness. Furthermore, the fact that it is not capable of full conversion of fuel is not a disadvantage; its use in the proposed composite was intended as a participating support alone. This is a unique behavior of CeO_2, which the traditional support materials, such as Al_2O_3 obviously lack. It is worth mentioning that ceria particles were seen fluidizing extremely well and appeared to behave like those made by spray drying, though they were not.

3.4. Reduction Experiments. To ascertain the reproducibility and performance reliability of the ceria- or GDC-supported materials, each composite oxygen carrier was subjected to several reduction and oxidation cycles. The Fe_2O_3- and Mn_3O_4-based carriers were examined at 950 °C for three redox cycles each, using syngas and methane as the fuel. The CuO-based materials on the other hand, were examined at 900 and 925 °C for three redox cycles at each temperature with methane as the fuel. The reason for not evaluating CuO-based systems at 950 °C is that in accordance with the Cu−O phase diagram, the oxidation of Cu_2O to CuO is just barely possible with p_{O_2} = 0.05 atm at 950 °C;[6] the oxidation of Cu_2O proceeds much more smoothly at lower temperatures.

The exit gas stream composition as a function of time during the reduction of COGDC carrier with CH_4 at 925 °C is illustrated in Figure 7.

As can be seen from Figure 7, the O_2 concentration does not drop to zero in the inert phase prior to fuel addition. This is ascribed to the release of gaseous oxygen via the so-called CLOU effect by the spontaneous decomposition of CuO into Cu_2O. The concentrations of CH_4 and CO drop to zero during reduction cycles, confirming complete conversion of the fuel into CO_2 with no detectable level of the fuel in the stream. There is also a considerable increase in the measured O_2 concentration, which is an artifact of measurement and gas analysis technique, as explained in the following. CH_4 in the fuel reactor is converted to CO_2 and H_2O via stoichiometric oxidation. Since oxidation of 1 mol of CH_4 produces 1 mol CO_2 and 2 mols H_2O, as high as three times flow could be expected. After the reactor, the gas is cooled down and steam removed by condensation, the volumetric flow is reduced roughly by a factor of 3, while that of CO_2 and O_2 will remain

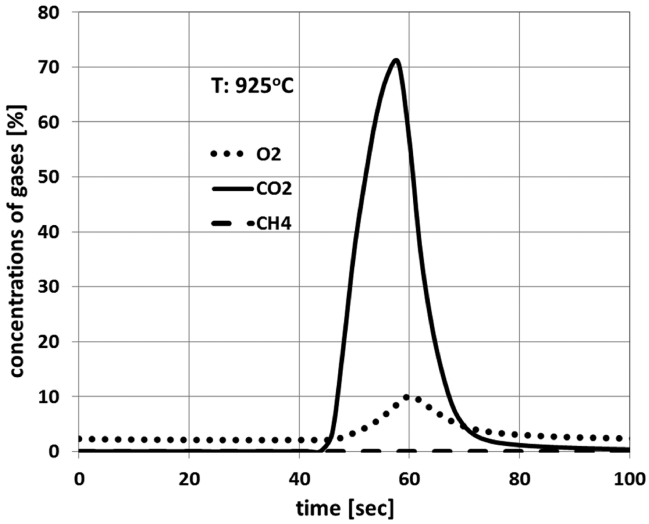

Figure 7. Time dependence profile of the exit gas stream for **COGDC** during reduction cycle using $\mathbf{CH_4}$ as fuel at 925 °C.

constant. For this reason, and if the rate of release of O_2 from the particles is rapid, the measured O_2 concentration could be expected to be three times as high as the equilibrium partial pressure. The measured increase is actually larger than expected because of condensation. This can be ascribed to the temperature increase during oxidation and subsequent increase in equilibrium partial pressure of oxygen.

It is important to compute the amount of oxygen used in the particles. This is done by using the mass-based conversion, ω, as defined in eq 5. The gas yield can be expressed as a function of solid conversion, as is illustrated for COC and COGDC particles at 900 and 925 °C in Figure 8 and for FOC and FOGDC particles at 950 °C in Figure 9.

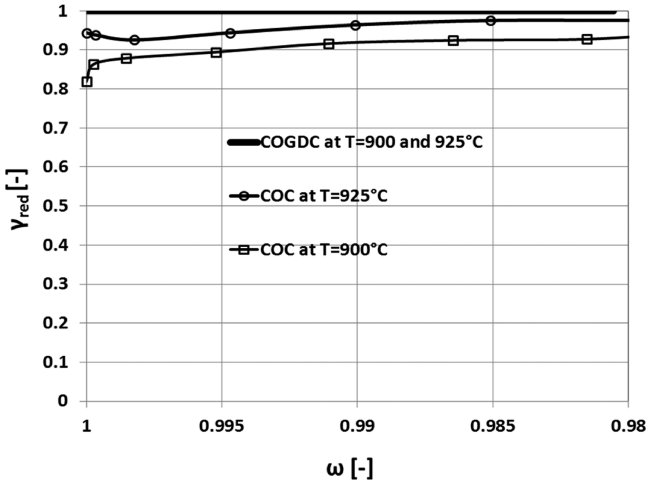

Figure 8. Gas yield as a function of conversion for the copper-based particles with a fuel flow of 900 mL/min $\mathbf{CH_4}$.

As can be seen from Figure 8, the reactivity of COC is quite high both at 900 and 925 °C. Moreover, the conversion of CH_4 increases slightly with time: up to ∼95% at 900 °C to ∼99% at 925 °C. Thus, as expected, CH_4 conversion is higher at higher temperature, reaching almost completion at 925 °C. COGDC converted CH_4 completely into CO_2 and H_2O both at 900 and 925 °C and the conversion remained stable with time. The

dx.doi.org/10.1021/ie300168j | Ind. Eng. Chem. Res. 2012, 51, 12796−12806

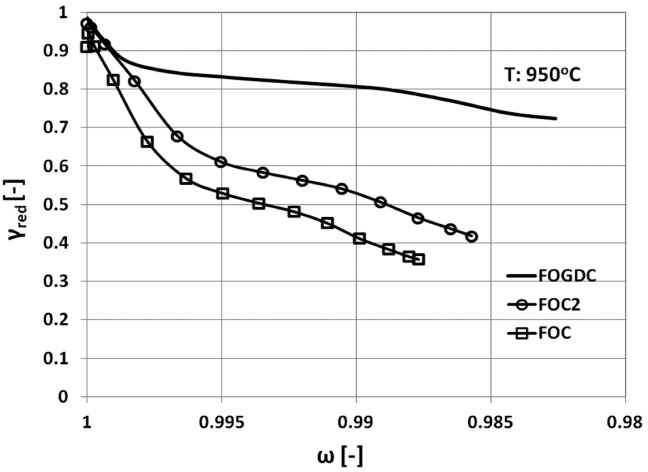

Figure 9. Gas yield as a function of conversion for the iron-based particles at 950 °C with CH_4 flowing at 450 mL/min.

performance of GDC-supported copper oxide particles is even better than that of the COC system.

As evident from Figure 9, CH_4 conversion was almost complete in the very beginning of the fuel cycle when Fe_2O_3-based carriers (FOC1, FOC2) were employed. However, the conversion decreased with time; this could be due to the depletion of oxygen in the carrier particles. Generally, iron particles are not capable of converting CH_4 completely into CO_2 and H_2O in the experimental setup used here, as has been seen in several previous studies.[16,17,23]

CeO_2 has higher density compared to alumina and other materials commonly used as support in CLC applications. Hence, the overall density of CeO_2-based formulations is also higher than those of more conventional oxygen carriers. Therefore, to maintain good fluidization and prevent agglomeration of material in the reactor bed, considerably higher flow rate of CH_4 (900 Ml/min; Table 2) was necessary while testing CuO-based particles. In addition, unlike spray drying or freeze granulation techniques, particles prepared by extrusion are not ensured to have very uniform geometry or high sphericity. The rather high fuel flow rate seems to be the reason why CH_4 was not fully converted by the COC oxygen carrier. Thus, the somewhat lower conversion of CH_4 at 900 °C compared to that at 925 °C could be a combined effect of temperature, particle shape as well as the high flow rate.

FOGDC oxygen carrier also showed better reactivity with CH_4 than those supported on pure CeO_2. About 88% CH_4 conversion was obtained by FOGDC for $\omega > 0.99$. It should be pointed out that such good performance has not previously been seen with Fe_2O_3-based carriers, using this particular reactor system and process parameters. This suggests that FOGDC could be a promising carrier for large scale chemical looping applications.

The average CH_4 conversion (γ_{red}) for the tested particles for a value of $\omega > 0.99$ is presented in Table 5.

The use of $\Delta\omega$ of 0.01 is reasonable with respect to the difference in solid conversion between air and fuel reactor in a CLC system.[27] The amount of oxygen transferred is directly related to the recirculation rate of the oxygen carrier, as well as the heat balance. As most reactions between hydrocarbon fuels and metal oxides are endothermic, the recirculation rate needs to be high enough to avoid too large temperature drops in the fuel reactor. Thus it is likely that only part of the active oxygen in the particle needs to be transferred, that is, a small $\Delta\omega$.

The syngas conversion for the iron- and manganese-based materials examined in this work was over 99.5%, as can be seen in Figure 10. The copper-based materials were not evaluated

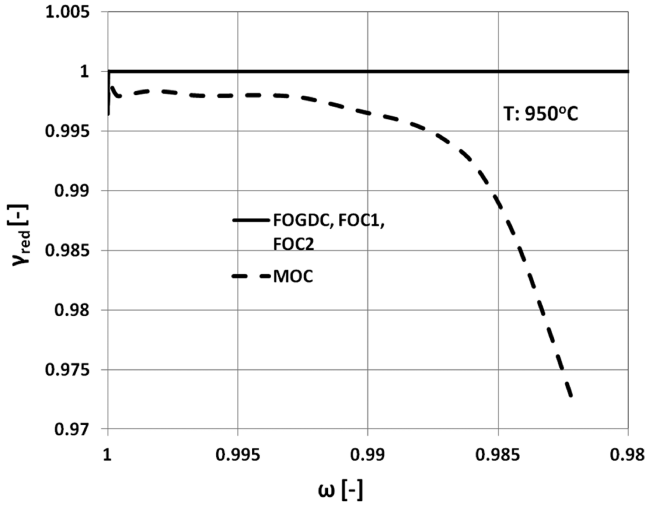

Figure 10. Mass-based conversion (ω) dependence of syngas conversion efficiency (γ) for FOC1, FOC2, FOGDC, and MOC at 950 °C with a fuel (syngas) flow rate of 450 mL/min.

with syngas as fuel, but since they caused near theoretical conversion of methane and the reactivity of solid oxygen carriers with syngas ($CO + H_2$) is an order of magnitude higher than that of CH_4, it is reasonable to expect that syngas too would undergo full conversion into CO_2 and H_2O.

In the case of ceria-supported Mn_2O_3 carrier (MOC) the gas yield was somewhat below 1 for the entire reduction period. From Table 5, the conversion of CH_4 by MOC was very low at 950 °C. This is surprising since manganese-based carriers are known to be efficient carriers[15] and typically provide good reactivity toward CH_4.[18,19] The thermodynamics in the light of Mn−O phase diagram suggest that oxidation of Mn_3O_4 to Mn_2O_3 is prohibited at 950 °C, which would limit the operation of the Mn-based carrier to the Mn_3O_4/MnO phase field. Reduced temperature could possibly facilitate oxidation to Mn_2O_3, thereby improving the reactivity and possibly result in O_2 release as well via CLOU effect. As mentioned earlier, no CLOU effect was observed for this material, irrespective of temperature, and additional experiments with methane at 800, 850, and 900 °C, showed no increase in reactivity, withthe CH_4 conversion, below 10% independent of temperature.

Table 5. Summary of CH_4 Conversion by the CeO_2- and $Ce_{0.9}Gd_{0.1}O_{1.9}$-Supported Oxygen Carriers for $\omega > 0.99$

	COC		FOC1	FOC2	MOC	FOGDC	COGDC	
temperature (°C)	900	925	950	950	950	950	900	925
CH_4 flow (mL/min)	900	900	450	450	450	450	900	900
CH_4 conversion (%)	88	95	68	74	<10	88	100	100

dx.doi.org/10.1021/ie300168j | Ind. Eng. Chem. Res. 2012, 51, 12796−12806

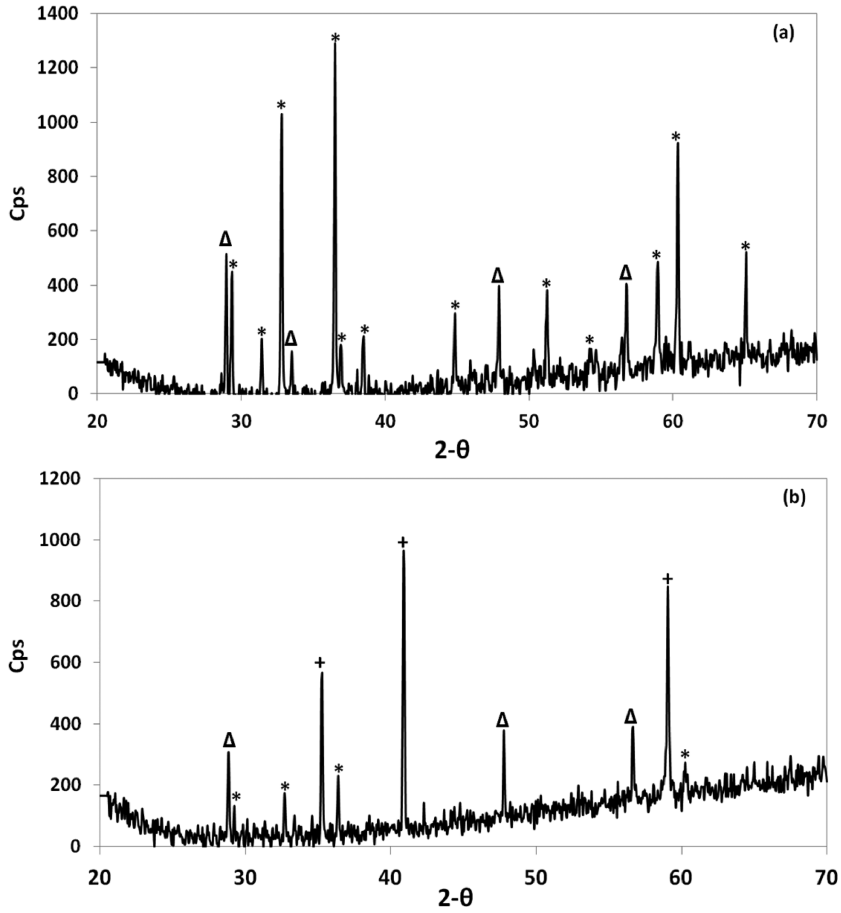

Figure 11. XRD patterns of the (a) as-prepared MOC, Mn_3O_4 (*) and CeO_2 (Δ). and (b) syngas reduced MOC, Mn_3O_4 (*),CeO_2 (Δ), and MnO (+).

The reason for the poor performance of MOC system is somewhat puzzling and unclear. Zhu et al.[28] have investigated cerium−manganese mixed oxides as oxidation catalysts. They claimed to have synthesized Mn-substituted CeO_2 ($Ce_{0.5}Mn_{0.5}O_{1.75}$ and $Ce_{0.8}Mn_{0.2}O_{1.9}$). But the XRD signatures reported by them are no different from those obtained in this work. Interestingly, they also observed peaks due to Mn_3O_4 during the test and attributed them to the transition from MnO to Mn_3O_4 during oxidation. It is worth pointing out that their attempt to oxidize Mn_3O_4 to Mn_2O_3 even in pure oxygen at 700 °C was not successful. It was stated that due to the presumed interaction between CeO_2 and Mn_3O_4, the MnO−Mn_3O_4 equilibrium oxygen partial pressure could have shifted to lower values. It therefore, appears that a similar interaction mechanism is operative in the MOC system investigated in this work, though the post-test XRD analysis of the MOC carrier gave no indication of the formation of Mn-doped ceria phases referred to by Zhu et al.[28] On the contrary, the only phases present in our samples were CeO_2 and Mn_3O_4. The XRD patterns of the as-prepared and syngas reduced forms of MOC particles are present in Figure 11. The diffraction signature of MOC particles reoxidized in 5% O_2 is identical to that of the as-prepared sample. The later refers to particles reduced by syngas at 950 °C for 25 s.

Irrespective of the method of preparation used (citric acid complexation by Zhu et al.[28] or the solid-state reaction in this work), it is rather difficult to make solid solutions, such as those claimed by Zhu et al.,[28] by mere calcination of powders at 700 °C for 5 h. Incorporation of manganese ions in CeO_2 lattice is a slow and diffusion-controlled process; it seems highly unlikely to occur at such low temperatures. Hence, in conclusion, it is believed that their claim of the formation of Mn-substituted CeO_2 compounds in the Mn_2O_3−CeO_2 system lacks irrefutably substantiative evidence. There appear to be a totally different reason for the rather poor performance exhibited by MOC carrier in this work and more detailed and systematic work is warranted to understand this behavior.

3.5. Oxidation Experiments. Focus of the current work has been on the reactions occurring in the fuel reactor of a chemical-looping combustor, though the oxidation reaction is also important to achieve a viable system. The reactor setup used here, however, is not optimized to study the oxidation reaction, which is often very fast. This means that in most of the cases, all the O_2 added to the reactor is consumed. Thus, obtaining a reaction rate that is not limited by O_2 concentration, is rather difficult. This aspect is true for the particles examined in this study as well. When flushed with a stream of 5% O_2 in N_2, the iron- and manganese-based particles initially consumed O_2 rather quickly. This is quite evident for the FOC2, FOGDC, and pure CeO_2 particles; in these cases, the O_2 concentration increased in a rather steep step from 0 to the saturation level of 5%, once the particles was fully oxidized (shown in Figures 4b and 6). Interestingly, the rate of increase in O_2 concentration from 0 to 5% at the end of the oxidation period for FOC1 and MOC was somewhat less sharp. Similarly, the reduced copper oxide particles were unable to consume all

dx.doi.org/10.1021/ie300168j | Ind. Eng. Chem. Res. 2012, 51, 12796−12806

Table 6. Summary of the Phase Analysis on the Post-Testing Reduced and Oxidized Oxygen Carriers

oxygen carrier	COC	COGDC	FOC1	FOC2	FOGDC	MOC
reducing gas	methane	methane	syngas	syngas	syngas	syngas
phases in reduced sample	Cu_2O, CuO, CeO_2	Cu_2O, Cu $Ce_{0.9}Gd_{0.1}O_{1.9}$	Fe_3O_4, CeO_2	Fe_3O_4, CeO_2	Fe_3O_4 $Ce_{0.9}Gd_{0.1}O_{1.9}$	MnO, Mn_3O_4 CeO_2
phases in oxidized sample	CuO, CeO_2	CuO $Ce_{0.9}Gd_{0.1}O_{1.9}$	Fe_2O_3, CeO_2	Fe_2O_3, CeO_2	Fe_2O_3 $Ce_{0.9}Gd_{0.1}O_{1.9}$	Mn_3O_4, CeO_2

O_2 during oxidation; in this case, they transform to their fully oxidized state gradually: a behavior that is commensurate with the theoretically predicted thermodynamic consideration of the phase relationships in the Cu−O system at and above 900 °C.

3.6. Fluidization and Agglomeration Characteristics. Feasibility of defluidization of the carrier particles in the reactor was monitored by measuring the pressure difference over the bed. However, all the oxygen carriers tested in this study showed good fluidization properties during successive oxidation and reduction cycles. No defluidization was observed except for the FOC1 particles, which defluidized after a long reduction cycle with syngas. This is not unusual and could be expected for oxygen carriers with high reactivity during long reduction cycles. This is particularly true for iron-based materials, which are prone to defluidization once wüstite (FeO) is formed.[15]

For FOC2, about 15% of the sample was found to have agglomerated. The agglomerates, however, were very soft and could be broken down by slight tapping of the reactor. Small agglomeration was observed in the case of COGDC particles as well. As can be seen from the XRD results in Table 6, metallic copper was formed in the reduced COGDC sample, which could have contributed to the observed agglomeration. Metallic copper has a low melting point and tends to make particles stick together, which then agglomerate. For other oxygen carriers, no sign of agglomeration was observed.

3.7. Post Redox Phase Analysis. At the end of the entire experimental protocol, two sets of XRD patterns were collected for each oxygen carriers. In one case, diffraction was conducted on fully oxidized particles by flushing the reactor with a 5% O_2−N_2 stream after the last reduction cycle. In the second case, XRD signature was collected on fully reduced (with methane in the case of copper-based and, with syngas in the case of iron- and manganese-based) particles. The duration of reduction period was chosen so as to reduce CuO to Cu_2O, Fe_2O_3 to Fe_3O_4, and Mn_2O_3 to Mn_3O_4 or MnO, assuming that the fuel conversion was 100%. These XRD results are summarized in Table 6.

The results conform to the phases expected in these carriers in both oxidized and reduced conditions. Moreover, there was no evidence of mutual interaction or formation of new compounds or solid solutions between the active material and CeO_2 in any case. This could be an advantage compared to the conventional support materials such as Al_2O_3, which for example can interact with CuO during sample synthesis and operation, resulting in partial loss of the active phase and complicating the phase relationships, recently reported by Arjmand et al.[29]

It is interesting to note that Mn_3O_4 rather than Mn_2O_3 was seen even in the fully oxidized MOC sample, which is understandable under the test conditions employed. The phases identified in the case of FOC and FODGC carriers were in accordance with their chemical state expected under reducing and oxidizing conditions in the reactor. Under the pO_2 conditions prevailing in the fuel reactor, though ceria (CeO_2) is likely to get reduced, it is by no means a bulk reduction (since the reduction cycle is too short). Therefore, it is rather impossible to detect minute reduced phase CeO_{2-x} (for example Ce_2O_3) in the XRD pattern, which as pointed out in Table 6, remains to be CeO_2. Same is true in the case of GDC as well.

Detection of elemental copper in the case of COGDC particles indicates that complete reduction of CuO was achieved. In comparison, there is still some CuO present and no metallic Cu in the COC sample. The likely explanation for this is that the higher reactivity of COGDC resulted in a higher degree of reduction.

4. CONCLUSION

The objective of this study has been to introduce and demonstrate the concept of a *participating* rather than *inert* support material for the application of solid oxygen carriers in chemical-looping combustion. This has been done by manufacturing and examination of ceria-based support materials in combination with the conventional transition metal oxides as oxygen carriers.

Particles of CuO, Fe_2O_3 and Mn_3O_4 supported on CeO_2 or $Ce_{0.9}Gd_{0.1}O_{1.9}$ were successfully manufactured by extrusion, and their performance was evaluated by reduction and oxidation experiments in a bench-scale batch fluidized bed reactor using CH_4 and syngas as fuel.

All materials showed good fluidization properties with no signs of sintering and little tendency toward agglomeration. CuO-based carriers had the highest reactivity with fuel and showed complete or nearly complete conversion of CH_4 into CO_2 and H_2O at 900−925 °C. CuO-based materials also released gas phase O_2 during fluidization with N_2, as well as during reduction with CH_4 as long as there was complete combustion of the fuel into CO_2 and H_2O. This suggests that these materials could be very interesting for chemical-looping combustion with O_2 uncoupling of solid fuels. In the case of Fe_2O_3-based carriers, up to 90% CH_4 conversion was achieved at 950 °C. Both CuO and Fe_2O_3 particles supported on$Ce_{0.9}Gd_{0.1}O_{1.9}$ were more reactive compared to those supported on pure CeO_2. The behavior of MOC particles was somewhat different, with rather low conversion of CH_4. Some explanation has been offered for their observed behavior in the light of thermodynamic consideration and the XRD results. The conversion of syngas was close to 100% for all examined materials.

Analysis of fresh and used particles by XRD did not reveal the formation of any unexpected phases. There was no evidence of mutual interaction or formation of new compounds or solid solutions between the active material and either of the two supports in any case.

It can be concluded that both CeO_2- and $Ce_{0.9}Gd_{0.1}O_{1.9}$-supported systems are promising oxygen carriers for chemical-looping applications, and that the use of participating support materials has potential to improve the performance of Fe_2O_3- and CuO-based oxygen carrier materials.

AUTHOR INFORMATION

Corresponding Author

*Tel.: +1 419 530 8103. E-mail: abdul-majeed.azad@utoledo.edu.

Notes

The authors declare no competing financial interest.

ACKNOWLEDGMENTS

The authors wish to thank Ian Richard, who participated in the preparation of oxygen carriers used in the study as a part of an Erasmus Scientific Project. One of the authors, Abdul-Majeed Azad, wishes to thank the United States Council for International Exchange of Scholars for the 2010−11 Fulbright Distinguished Chair Award in Alternative Energy Technology, which facilitated his stay and collaboration with the chemical-looping group at Chalmers in Sweden.

REFERENCES

(1) Lewis, K. W.; Gilliland, E. R.; Sweeney, M. P. Gasification of carbon: Metal oxides in a fluidized powder bed. *Chem. Eng. Prog.* **1951**, *47*, 251−256.

(2) Hossain, M; De Lasa, H. Chemical-looping combustion (CLC) for inherent CO_2 separation—A review. *Chem. Eng. Sci.* **2008**, *63*, 4433−4451.

(3) He, F.; Li, H.; Zhao, Z. Advancements in development of chemical-looping combustion. *Int. J. Chem. Eng.* **2009**, No. 710515:1−16.

(4) Lyngfelt, A. Oxygen carriers for chemical-looping combustion—4000 h of operational experience. *Oil Gas Sci. Technol.* **2011**, *66*, 161−172.

(5) Moghtaderi, B. Review of the recent chemical looping process developments for novel energy and fuel applications. *Energy Fuels* **2012**, *26*, 15−40.

(6) Leion, H; Lyngfelt, A; Mattisson, T. Solid fuels in chemical-looping combustion. *Int. J. Greenhouse Gas Control* **2008**, *2*, 180−193.

(7) Mattisson, T; Leion, H; Lyngfelt, A. Chemical-looping with oxygen uncoupling using CuO/ZrO_2 with petroleum coke. Fuel 2009; 88, 683−690. (b) Leion H, Mattisson T, Lyngfelt A. Using chemical-looping with oxygen uncoupling (CLOU) for combustion of six different solid fuels. *Energy Proc.* **2009**, *1*, 447−453.

(8) Jerndal, E; Mattisson, T; Lyngfelt, A. Thermal analysis of chemical-looping combustion. *Chem. Eng. Res. Des.* **2006**, *84*, 795−806.

(9) Pröll, T; Mayer, K; Bolhàr-Nordenkampf, J; Kolbitsch, P; Mattisson, T; Lyngfelt, A; Hofbauer, H. Natural minerals as oxygen carriers for chemical-looping combustion in a dual circulating fluidized bed system. *Energy Proc.* **2009**, *1*, 27−34.

(10) Gayán, P; Forero, C. R.; Abad, A; de Diego, L. F.; García-Labiano, F; Adánez, J. Effect of support on the behavior of Cu-based oxygen carriers during long-term CLC operation at temperatures above 1073 K. *Energy Fuels* **2001**, *25*, 1316−1326.

(11) Chuang, S. Y.; Dennis, J. S.; Hayhurst, A. N.; Scott, S. A. Development and performance of Cu-based oxygen carriers for chemical-looping combustion. *Combust. Flame* **2008**, *154*, 109−121.

(12) de Diego, L. F.; García-Labiano, F; Gayán, P; Celaya, J; Palacios, J. M.; Adánez, J Operation of a 10 KWth chemical-looping combustor during 200 h with a Cu-Al_2O_3 oxygen carrier. *Fuel* **2007**, *86*, 1036−1045.

(13) Forero, C. R.; Gayán, P; de Diego, L. F.; Abad, A; García-Labiano, F; Adánez, J. Syngas combustion in a 500 Wth chemical-looping combustion system using an impregnated Cu-based oxygen carrier. *Fuel Process. Technol.* **2009**, *90*, 1471−1479.

(14) Abad, A; Mattisson, T; Lyngfelt, A; Johansson, M. The use of iron oxide as oxygen carrier in a chemical-looping reactor. *Fuel* **2007**, *86*, 1021−1035.

(15) Cho, P; Mattisson, T; Lyngfelt, A. Defluidization conditions for a fluidized bed of iron oxide-, nickel oxide-, and manganese oxide-containing oxygen carriers for chemical-looping combustion. *Ind. Eng. Chem.* **2006**, *45*, 968−977.

(16) Rydén, M; Cleverstam, E; Johansson, M; Lyngfelt, A; Mattisson, T. Fe_2O_3 on Ce-, Ca-, or Mg-stabilized ZrO_2 as oxygen carrier for chemical-looping combustion using NiO as additive. *AIChE J.* **2010**, *56*, 2211−2220.

(17) Rydén, M; Cleverstam, E; Lyngfelt, A; Mattisson, T. Waste products from the steel industry with NiO as additive as oxygen carrier for chemical-looping combustion. *Int. J. Greenhouse Gas Control* **2009**, *3*, 693−703.

(18) Leion, H; Mattisson, T; Lyngfelt, A. Use of ores and industrial products as oxygen carriers in chemical-looping combustion. *Energy Fuels* **2009**, *23*, 2307−2315.

(19) Johansson, M; Mattisson, T; Lyngfelt, A. Investigation of Mn_3O_4 with stabilized ZrO_2 for chemical-looping combustion. *Chem. Eng. Res. Des.* **2006**, *84*, 807−818.

(20) Abad, A; Mattisson, T; Lyngfelt, A; Ryden, M. Chemical-looping combustion in a 300 W continuously operating reactor system using a manganese-based oxygen carrier. *Fuel* **2006**, *85*, 1174−1185.

(21) Rydén, M; Lyngfelt, A.; Mattisson, T. Combined manganese/iron oxides as oxygen carrier for chemical-looping combustion with oxygen uncoupling (CLOU) in a circulating fluidized bed reactor system. *Energy Proc.* **2011**, *4*, 341−348.

(22) Azimi, G; Leion, H; Mattisson, T; Lyngfelt, A. Chemical-looping with oxygen uncoupling using combined Mn-Fe oxides, testing in batch fluidized bed. *Energy Proc.* **2011**, *4*, 370−377.

(23) Leion, H; Larring, Y; Bakken, E; Mattisson, T; Bredesen, R; Lyngfelt, A. The use of $CaMn_{0.875}Ti_{0.125}O_3$ as oxygen carrier in chemical-looping with oxygen uncoupling (CLOU). *Energy Fuels* **2009**, *23*, 5276−5283.

(24) Rydén, M; Lyngfelt, A; Mattisson, T. $CaMn_{0.875}Ti_{0.125}O_3$ as oxygen carrier for chemical-looping combustion with oxygen uncoupling (CLOU)−experiments in a continuously operating fluidized bed reactor system. *Int. J. Greenhouse Gas Control* **2011**, *5*, 356−366.

(25) Sundararajan, D; Azad, A. M. Cooperative synergy in nanoscale ceria-based systems. *Sci. Adv. Mater.* **2011**, *3*, 739−762.

(26) Metselaar, R; van Tol, R. E. J.; Piercy, P. J. The electrical conductivity and thermoelectric power of Mn_3O_4 at high temperatures. *Solid State Chem.* **1981**, *38*, 335−341.

(27) Mattisson, T; Järdnäs, A; Lyngfelt, A. Reactivity of some metal oxides supported on alumina with alternating methane and oxygen—Application for chemical-looping combustion. *Energy Fuels* **2003**, *17*, 643−651.

(28) Zhou, G; Shah, P. R; Gorte, R. J. Study of cerium−manganese mixed oxides for oxidation catalysis. *Catal. Lett.* **2008**, *120*, 191−197.

(29) Arjmand, M; Azad, A.-M.; Leion, H; Lyngfelt, A; Mattisson, T. Prospects of Al_2O_3 and $MgAl_2O_4$-supported CuO oxygen carriers in chemical-looping combustion (CLC) and chemical-looping with oxygen uncoupling (CLOU). *Energy Fuels* **2011**, *25*, 5493−5502.